Journal of Radiation and Nuclear Applications
An International Journal

http://dx.doi.org/10.18576/jrna/070101

Geology and Radioactivity of the Pegmatitic Rocks of Gabal El Urf, Northern Eastern Desert, Egypt

El Dabe, M. M, Ismail, A. M [*] *and Metwaly M*

Nuclear Materials Authority, P.O. Box: 530, Maadi, Cairo, Egypt.

Received: 22 Sep. 2021, Revised: 2 Oct. 2021, Accepted: 25 Nov. 2021.
Published online: 1 Jan 2022.

Abstract: The pegmatitic rocks that intrude Monzogranites of Gabal El Urf, North Eastern Desert, are characterized by poly-phased mineralization. It is located southwest of the granitic pluton and consisting of three zones; the outer one is represented by potash feldspar, the middle by quartz, and the inner occupied with mica and accessory minerals. Two phases of mineralization are recorded; the earlier is characterized by colorful mineralization**,** nearly located at the inner zone along the N-S and intersection area between NE-SW and NW-SE trends. The latter is characterized by the dominance of opaque minerals spreading in the three zones of the pegmatite along with the NE-SW and E-W trends and filling the fractures. The earlier phase is characterized by the presence of radioactive minerals (thorite, xenotime, and zircon). The later phase is characterized by another array of accessory minerals (fluorapatite, cassiterite, atacamite, sulfides and Nb-minerals) beside the Th-minerals (thorite, uranothorite,), U-minerals (autunite and uranophane), REE-bearing minerals (pyrochlore and bastnasite) and iron oxides minerals. It possesses a net of fractures filled by iron oxides associated with the transported uranium and REE's. There are two levels of radioactivity; the first one is moderate (eU 26 ppm - eTh 245 ppm) and the second is (eU 45 ppm, eTh 1061 ppm) on average. Radioactivity of El Urf pegmatitic rocks is syngenetic and related to the late-stage magmatism, proved by the high Th-concentrations and presence of the radioactive minerals, followed by uranium migration. The high concentrations of thorium and the high values of Th/U ratio in the radioactive pegmatitic rocks rather than the world (3.5) indicated that the uranium migrated from a zone to another in the same pegmatite by a circulating hydrothermal solution.

Keywords: Gabal El Urf, zoned pegmatite, Radioactive minerals.

1 Introduction

The investigated pegmatite is located in the southwestern part of Gabal El Urf in the North Eastern Desert of Egypt between latitudes 26° 37′ 58′′– 26° 38′ 11′′ N and longitudes 33° 26′ 51′′– 33° 28′ 09′′ E (Fig. 1). In general, Gabal El Urf area, which includes the El Urf younger granites pluton and related pegmatitic rocks, has interesting chemical and mineralogical characteristics.

Gabal El Urf had a lot of attention since the mid-nineteenth century. It is mainly monzogranite with calc-alkaline nature and Sr-Nd age of 600 ±11Ma, while the perthitic leucocratic and riebeckite type is generated from an alkaline magma [1],[2],[3] The diorite and granodiorite rocks represent as country rocks of the El Urf granite area and they enclose several mineralized pegmatites bodies [3]. Some dyke-like bodies are dissecting the granodiorite of Gabal El Urf [4]. Two bodies of Gabal El Urf pegmatites, Wadi Abu Shihat and Wadi Abu Zawal, were revealed to be mineralized by uranium and thorium. [5],[6].

Gabal El Urf zoned pegmatites are composed of quartz-rich in the core, mica-rich in the middle zone, and a feldspar-rich wall zone. These three zones of pegmatites constitute a source for radioactive and rare metals (Y, Th, Nb, and Zr) mineralization. [7]. In general, all pegmatite rocks in Gabal El Urf younger granite have been recorded in their country rocks (diorite and granodiorite). The pegmatites derived from metaluminous to peralkaline magma and fall within plate granite type and enriched of cheralite (Ca-rich monazite) and zircon [4]. They had strongly affected by hydrothermal processes enriched with rare metals mineralization, especially copper anomaly accompanied with intense tectonic structure [7]. Many radioactive minerals are recorded in the mineralized

[*]Corresponding author e-mail: a.m.ismail302@gmail.com

pegmatite area as thorianite, columbite, and uranophane [3]. The pegmatites which containing rare minerals and originated from late-stage hydrothermal fluids are called complex pegmatites [8].

[9] have experimentally modeled the origin of pegmatite-aplite bodies and notifying that fine-grained feldspar and quartz had crystallized on the walls of the closed system whereas the core was comprised of much larger crystals. They explained that the system became saturated with water after the initial crystallization of the anhydrous minerals (feldspar and quartz). Consequently, a fine-grained aplite margin had been created retrograding the boiling and then created a separate aqueous phase in which the large crystals readily grew. They concluded that the parental magma of most granitic pegmatites crystallizes in three main stages:

a) Crystallization of essentially anhydrous minerals such as the feldspars and quartz. b) Crystallization of minerals from both a silicate liquid and coexisting aqueous fluid of considerably lower viscosity followed by rapid diffusion of constituents through the aqueous fluid and the upward movement of the fluid phase. All contribute to the formation of pods and zones of different compositions and textures. c) Crystallization and metasomatism by aqueous fluids after the crystallization of the silicate liquid.

The present study is concerning with the geology and radioactivity of the pegmatitic rocks intruding Gabal El Urf monzogranites to throw light on their petrographical features, mineralogical composition, and recognize the minerals that responsible for their radioactivity.

2 Experimental Methods

2.1 Sample Measurement and Analysis

The field radiometric survey of the El Urf younger granite and its related pegmatite was carried out using the portable scintillometer (UG-130), measuring in terms of count per second (Cps) and determined also as equivalent uranium (eU) and thorium (eTh).
The petrography studies were mainly examined by A Nickon polarized microscope to recognize the radioactive minerals and radioelement-bearing minerals of the studied mineralized pegmatite.
X-ray diffraction technique (XRD), using Philips PW 3710/31 diffractometer, scintillation counter, Cr & Cu target tube, and Ni filter at 40 KV and 30 MA. This instrument is connected to a computer system using the APD program and PDF-2 database for mineral identification.
An Environmental Scanning-Electron Microscope (ESEM model Philips XL30) supported by an energy dispersive spectrometer (EDX) unit was used at 25-30 KV accelerating voltage, 1-2 mm beam diameter, and 60-120 second counting time. All the analyses were carried out at the labs of NMA, Egypt

2.2 Geological Setting

Gabal El Urf was exposed as an elongated mass of younger granite in NNE-SSW direction. It is pink in color, medium to coarse-grained, moderate to high topography. El Urf monzogranite intrudes metavolcanics, older granitoids and metagabbro with sharp contacts [2][7]. Pegmatites are intruded mainly in the country rocks **(Fig. 1)**. It is highly sheared and dissected by numerous faults and by several felsic and basic dykes in different directions. El Urf monzogranite indicates ages of 600±11 Ma, while its country rocks (granodiorite) showing 650±95 Ma [2].

The studied mineralized pegmatite is located in the extreme western part of Gabal El Urf **(Figs. 1 and 2)**. It is huge and irregular with elliptical extension; characterized by an extraordinarily well-developed zonation consisting of potash feldspar as outer zone, followed by quartz as middle zone, and finally mica as inner zone **(Fig. 3)**. The middle and inner zones are characterized by U-mineralization where quartz varies from clear white to smoky colors. Structurally, the investigated pegmatite has many joints and fractures; following NE-SW, NW-SE trends with lesser abundant N-S and NWW-SEE trends.

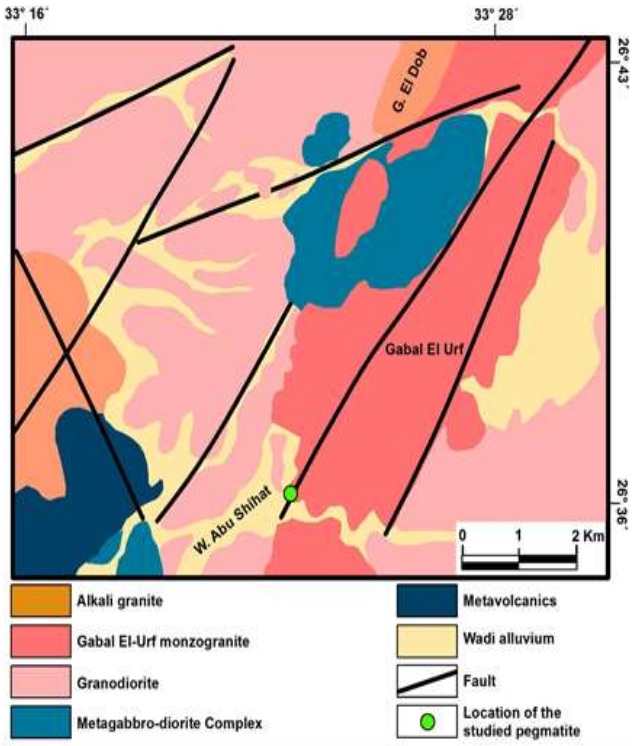

Fig. 1: Geological map of Gabal El Urf, North Eastern Desert, Egypt, modified after (Moghazi 1999), showing the location of the studied pegmatite.

Fig. 2: A panorama view showing a mineralized pegmatite intruding the younger granite of Gabal El Urf, looking NW.

The field studies indicated two phases of mineralization with two levels of radioactivity. The first phase (phase-I) exhibited a moderate radioactivity value, while the second phase (phase-II) is characterized by anomalous radioactivity **(Fig. 4)**.

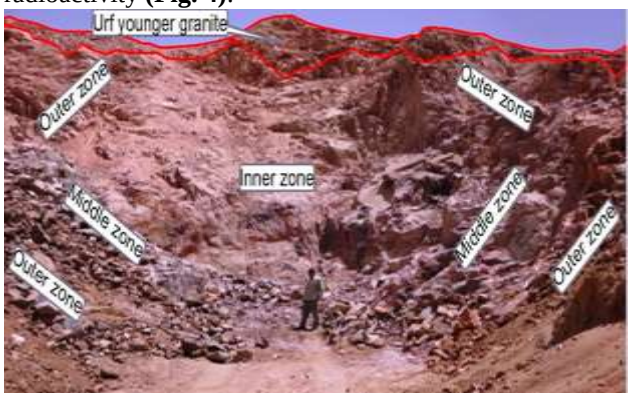

Figure 3 A close view of the mineralized zoned pegmatites intruding Gabal El Urf granite, looking N.

3 Results and Discussion

3.1 U- mineralization

Generally, the zone of potash feldspar is the largest zone rather than the quartz and mica zones. It received the majority of the hydrothermal solution charges. Mineralization has multi-stages and is distributed along the three zones as i) Colorful disseminated spots occupied by radioelement-bearing mineral crystals (phase-I) and ii) Small patches and thin films marked by iron oxides filling the cavities, joints, and fractures (phase-II) **(Fig. 4)**. Both phase-I and phase-II are distributed within the whole of the pegmatitic rocks.

The colorful phase-I occurs as clots of disseminated minute crystals with bright colors in quartz and potash feldspar **(Fig. 5)**. Generally, the coloration ranges from yellow, orange to green which is due to the type and quantity of the disseminated minerals and their alteration products.

The opaque mineralization phase-II is more spreading than the earlier mineralization phase-I consisting mainly of iron oxides and fluorite minerals associated with highly radioactive minerals **(Fig. 6)**. Mineralization of this phase occurs in different shapes varying from small cavities to mineral-filled fractures **(Fig. 7)**, sheet-like bodies along with the fractures and bands with variable sizes **(Fig. 8)**.

Structurally, the colorful mineralization phase-I is mainly located near or along the N-S and at the intersection area between NE-SW and NW-SE trends. While the later opaque phase-II is nearly spread in all three mineralized pegmatite zones. It invaded NE-SW and nearly E-W trends. The crosscut relation between the previous two radioactive mineralization phases (phase-I and phase-II) was recorded in some locations in the studied mineralized zoned pegmatite **(Fig.7 and Fig. 8)**.

3.2 Petrography

Eight samples were prepared as thin sections and examined by a polarized microscope to recognize the radioactive minerals and radioelement-bearing minerals. Generally, the accessory minerals are mostly found in the pegmatitic feldspar as fluorite, xenotime, and zircon beside the radioactive minerals. Microscopic investigation revealed that the zone of potash feldspar is composed mainly of megacrysts of rod-perthite **(Fig. 9)**. They occur as anhedral crystals of very coarse grain size (pegmatitic) up to 3.2 cm enclosing most of the accessory minerals. They are affected by the post-magmatic activity and traversed by several fractures filled by iron oxides **(Fig. 9)**. They are blended with the radioactivity that belongs to the second phase-II and sericitized along the two sides of the fracture by the thermal action of the hydrothermal solution **(Fig. 10)**.

Fluorite is the most abundant accessory mineral. There are two generations of fluorite; the first is magmatic that belongs to the late magmatic stage occurring as large crystals (up to 2.0 Cm). It is characterized by purple to violet colors **(Fig. 11)**; it corrodes the biotite flakes and encloses crystals of earlier minerals. Mostly; it is also associated with the hydrous radioactive minerals especially autunite and uranothorite **(Fig. 12)**. The second latter generation occurs in the veinlets of iron oxides cutting the earlier minerals (xenotime) **(Fig. 13)**.

Xenotime occurs as tetragonal crystals with bipyramidal form exhibiting its characteristic interference color. It is found associating the iron oxides **(Fig. 14)**, zircon and perthite; partially or completely metamectized referring to the presence of the radioelement and radioactive damage **(Fig. 15)** It is affected by the post-magmatic tectonism fractured and dislocated along the gliding plane **(Fig. 16)**.

Zircon is present as small crystals of a tetragonal system exhibiting its characteristic interference colors of the third order and is commonly associated with xenotime **(Fig. 17)**. Occasionally they are partially metamictized when they are surrounded by the iron oxides referring to the presence of the radioelements in zircon crystals **(Fig. 18)**.

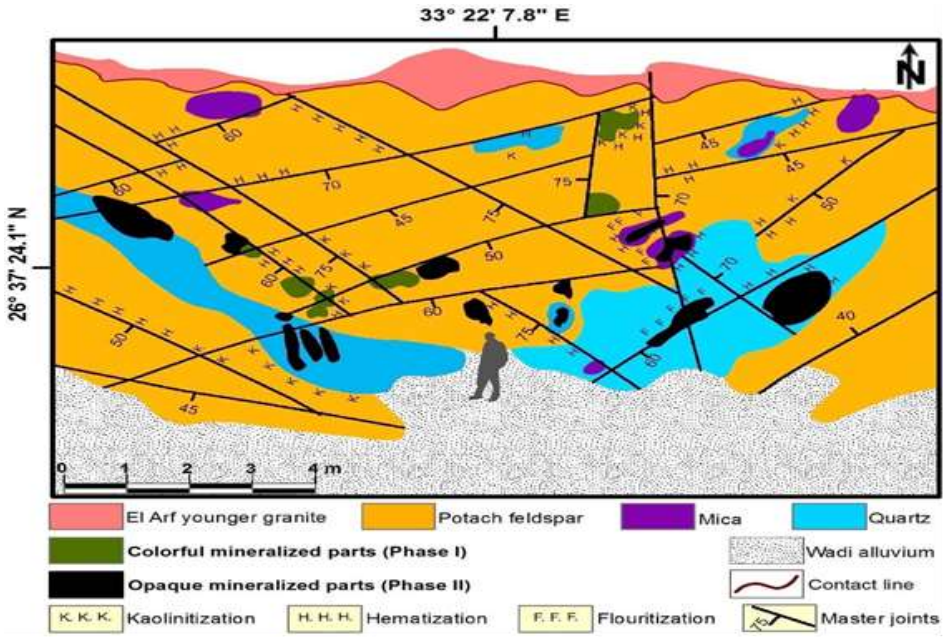

Fig. 4: A sketch for the studied pegmatites, southwest of the G. El Urf monzogranite, Showing the structural framework of G. El Urf and zoning of the pegmatites.

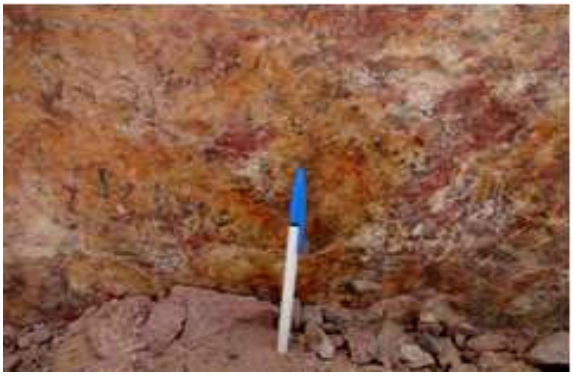

Fig. 5: Patches of bright yellowish colorful radioactive minerals (phase-I), staining potash feldspar surface, mineralized pegmatites, of Gabal El Urf area, looking NW

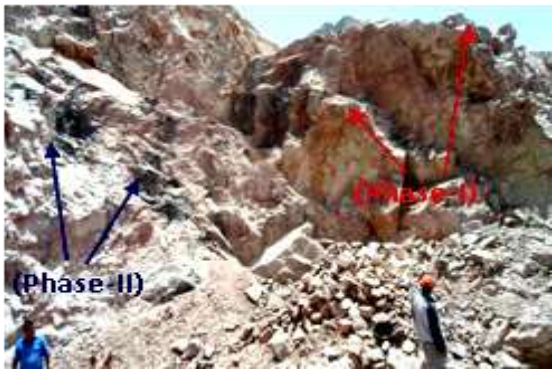

Fig. 6: Close up view clarifying the two phases (Phase-I and Phase-II), in the mineralized pegmatite, of Gabal El Urf area, Looking NE.

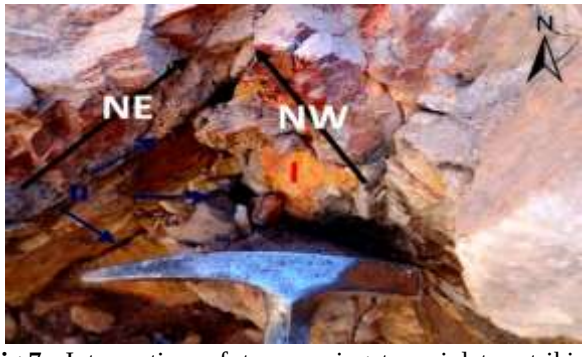

Fig.7: Intersection of two conjugate veinlets, striking NE-SW and NW-SE trends marked by iron oxides and fluorite, and associated with black radioactive minerals (phase-II), surrounding a spot of colorful radioactive minerals (phase-I).

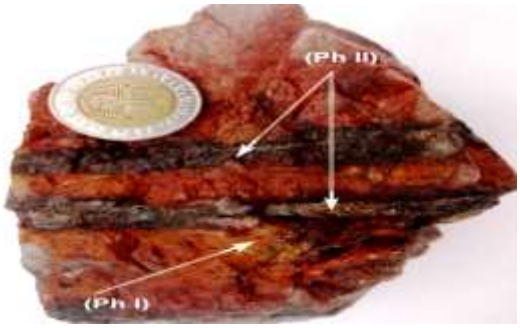

Fig. 8: A hand specimen showing parallel bands of iron oxides with high radioactivity (phase-II), cut across patch-shaped colorful radioactive minerals (phase-I). Mineralized pegmatite of Gabal El Urf area.

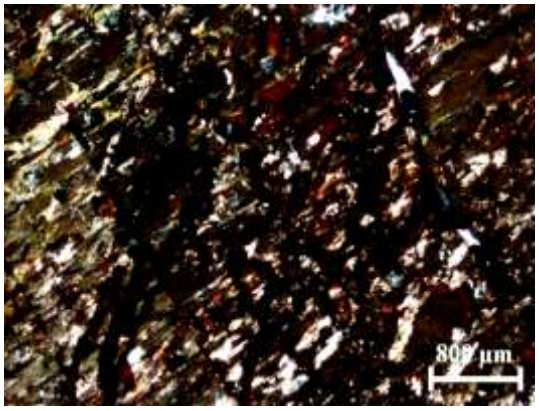

Fig. 9: Megacryst of perthite cut by net fractures filled by iron oxides, mineralized pegmatite of Gabal El Urf area, C.N.

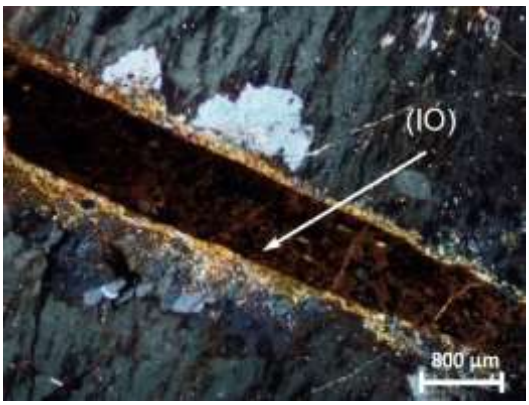

Fig. 10: Megacryst of rod perthite cut by fracture-filled with iron oxides blended with the trace elements, mineralized pegmatite of Gabal El Urf area, C.N.

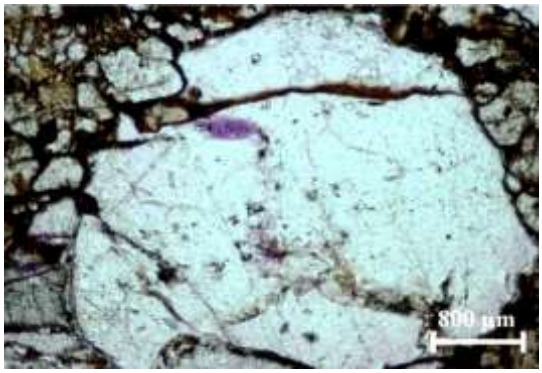

Fig.11: Coarse crystal of purple fluorite (Flu) (phase-I), cut by iron oxides and surrounded by granulated potash feldspar, mineralized pegmatite of Gabal El Urf area, C.N.

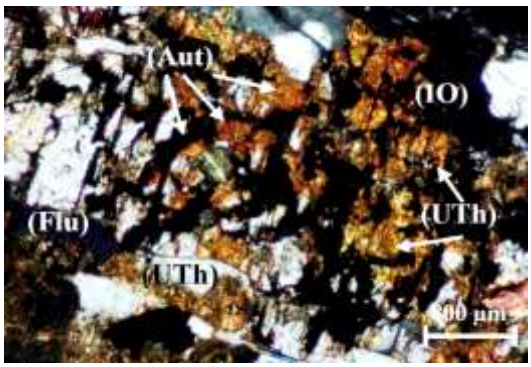

Fig.12: Rose-like crystals of autunite (Aut) (phase-I) associating uranothorite (UTh) and fluorite crystal (Flu), mineralized pegmatite of Gabal El Urf area, C.N.

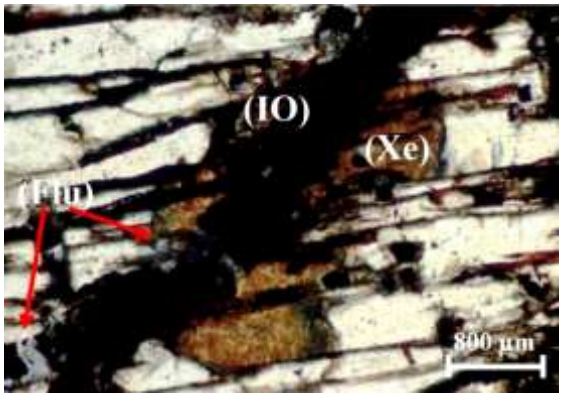

Fig.13: Xenotime (Xe) cut by fracture-filled with iron oxides (IO) and fluorite (Flu) of the second generation**,** min. peg. of G. El Urf area, C.N.

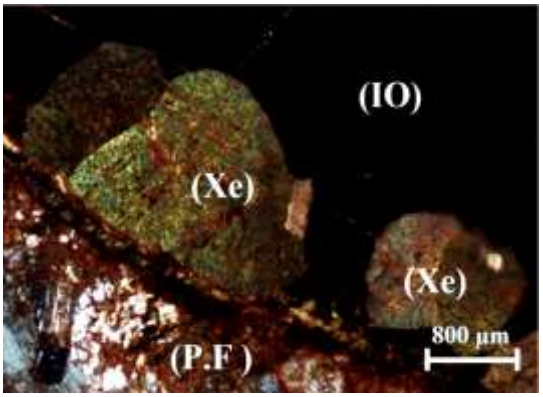

Fig.14: Euhedral crystals of xenotime (Xe) on the borders between potash feldspar (P.F) and iron oxides (IO), min. eg. of G.El Urf area, C.N.

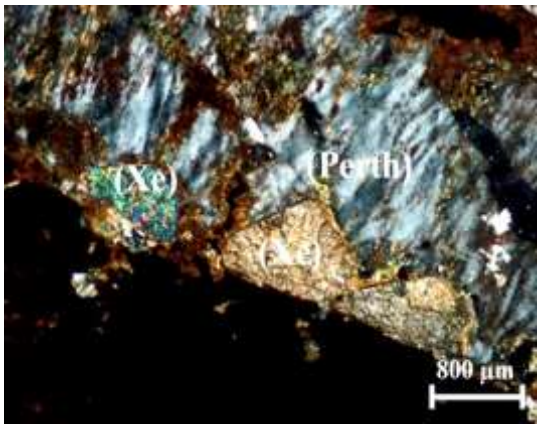

Fig.15: Partially and completely metamectized xenotime crystals (Xe) (phase-I) enclosed in perthite (Perth)**,** mineralized pegmatite, C.N.

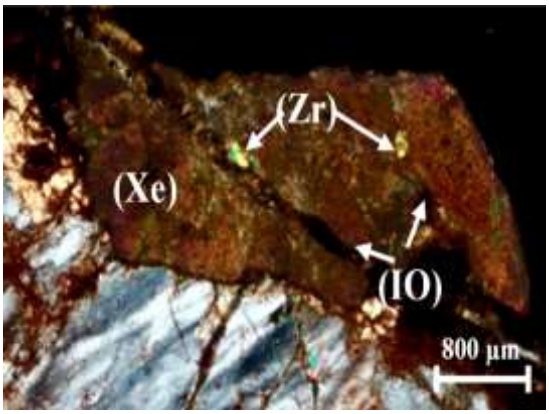

Fig. 16: Dislocation in a coarse crystal of xenotime (Xe) along gliding plane filled with iron oxides (IO), mineralized pegmatite, C.N.

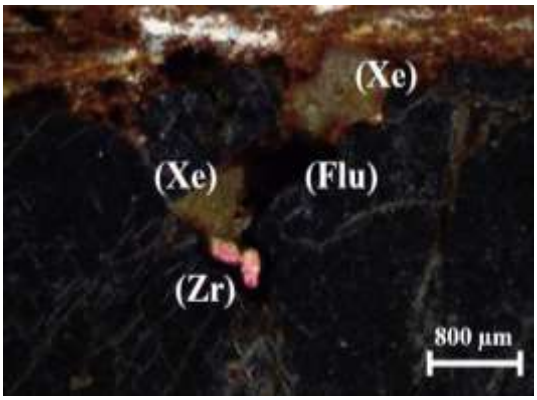

Fig.17: Minute crystals of zircon (Zr) associating xenotime (Xe) and fluorite (F) mineralized pegmatite of Gabal El Urf area, C.N.

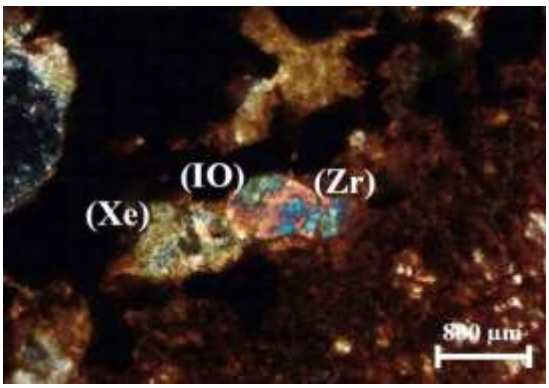

Fig.18: Fine crystals of zircon (Zr) and xenotime (Xe) surrounded by iron oxides (IO) mineralized pegmatite, C.N.

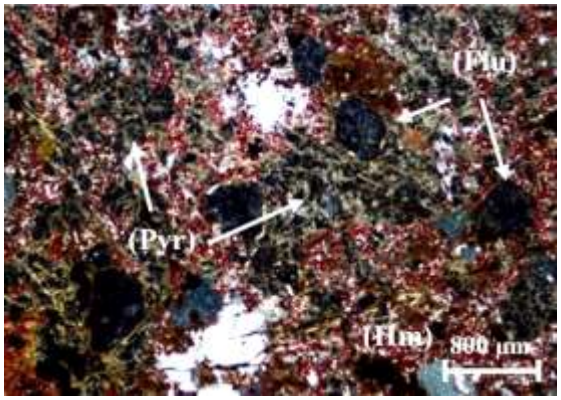

Fig. 19: Fluorite (F) and pyrochlore (Pyr) (phase-II), mineralized pegmatite of Gabal El Urf area, C.N.

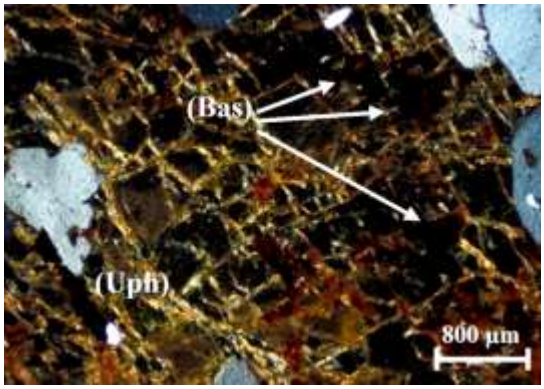

Fig.20: Veinlets of uranophane (Uph) associated with small dark brown bastnasite crystals (Bas) (phase-II), min. peg. of Gabal El Urf area, C.N.

The radioactive minerals recorded microscopically as phase-II are uranothorite, uranophane, pyrochlore, and bastnasite.

Uranothorite present as medium crystals with orange to green in color, exhibiting worm-like forms **(Fig. 12)**. Pyrochlore occurs as isolated medium opaque (isotropic) black to brown minerals surrounded by hematite and associated with purple fluorite and hematite **(Fig. 19)**. Amorphous uranophane is also present as network of bright yellowish threads commonly associated with bastnasite and fluorite **(Fig. 20)**. Bastnasite is an REE-bearing mineral; it occurs as small subhedral to euhedral dark brown crystals associated with uraonophan **(Fig. 20)**.

3.3 Radioactivity

The concentrations of radioelements in El Urf younger granite and its related mineralized pegmatite have been listed in **Table (1)** and the levels of radioactivity are illustrated as a histogram **(Figs. 21).**

El Urf younger granite occurs as a long thin strip associated mainly with kaolinization feature type located at the north of the studied mineralized pegmatite **(Figs. 2 & 4)**. Its total count (Tc) radioactive values range from 30 to a maximum value of 100 cps near the contact with the mineralized zoned pegmatite with an average equivalent (eU) and (eTh) values equal 2.72 and 7.40 ppm, respectively **(Table 1)**.

The studied mineralized pegmatite has a vast array of measuring radioactivity values varying from barren pegmatite to moderate and anomalous pegmatites **(Table 1)**. The barren pegmatite is ranging from 73.5 to 146.4 Tc with an average of 110.41 Tc. It possesses an average (eU) equal 7.50 and average (eTh) equal 19.19 ppm with Th/U ratio up to 3.22 approaching the world value (3-4), **(Table 1)**. The mineralized pegmatite could be categorized to moderately radioactive phase (phase-I), and anomalous phase (phase-II).

Geochemical facies could be determined using the eTh/eU ratio. Depending on the analyses of different rock samples, oxidizing or reducing conditions may be detected from the thorium to- uranium ratio [10-12]. under reducing conditions, uranium has an insoluble tetravalent state that is fixed, but under oxidizing conditions uranium is transformed to the soluble form which may be mobilized into solution. On the other hand, thorium has only insoluble tetravalent state. Geochemically, thorium is copartner with uranium, so, help in determination of geochemical conditions [13] [14]. Th/U ratios <2 are indicative of uranium enrichment while ratios >7 suggestive uranium removal or leaching.

The first group of pegmatite is characterized by e(U) ranging from 16.74 to 40.3ppm, with an average of 25.90 ppm and average (eTh) equal 245.46 ppm with an average Th/U ratio equal 9.18 **(Table 1)**. While the second group has e(U) values ranges from 29.41 ppm to 61.58 ppm with an average of 45.26 and average (eTh) equal 1061.63 ppm with an average Th/U ratio of 23.46 **(Table 1)**. Both of them have a higher ratio than the world ratio referring to uranium migration.

Generally, thorium concentrations in the studied rocks are high (up to 1419 ppm) accompanied by high magmatic uranium concentrations leading to the formation of the radioactive minerals, at the same time the studied rocks are characterized by very high Th/U ratios referring to the migration of the uranium. This may clarify that, the first pegmatite group may crystallize in oxidation-reduction conditions, in contrast to the second pegmatite group crystallize in highly excessive oxidation conditions.

The radiometric data is also expressed as a histogram indicating the three levels of radioactivity. The barren level comprises El Urf monzogranite and a part of the pegmatite while the moderate level is exhibited by the pegmatite with colorful mineralization (phase-I) and the anomalous level exhibited by the pegmatite with opaque mineralization (phase-II) **(Fig. 21)**. Plotting of eTh concentrations versus eTh/eU ratios indicated two cases, for the monzogranite and its related pegmatitic rocks **(Fig. 22)**.

Firstly, the monzogranite and the Phase-II of the pegmatitic rocks are characterized by scattered relationships with nearly horizontal regression lines and low correlation coefficients (r = 0.02 and r = 0.09), respectively. Secondly, the barren pegmatitic rocks and phase-I are characterized by positive relationships with moderate and high correlation coefficients values (r =0.52 and r =0.99), respectively **(Fig. 22)**. Positive correlation are indicative of magmatic processes whereas ill-trends clarify the effect of post-magmatic processes and refer to migration of uranium from these rocks [15-18].

3.4 Mineralogy of phase-I

The radioactivity of this phase is restricted to the mica minerals that include an array of radioelement-bearing minerals as xenotime, zircon and fluorite, in addition to thorite as the main radioactive mineral. The mica minerals are recognized by X-ray diffraction as biotite and phlogopite **(Fig. 23)**.

The minerals that are related to radioactivity are separated and examined by an electron scanning microscope as following:

3.4.1 Thorite ($(Th,U)SiO_4$)

Thorite is the main radioactive mineral that is present in this phase as minute grains included in the mica minerals and as fracture filling. It exhibits its characteristic ESEM

spectrograph and its composition is confirmed by EDX-analysis, thorium (35.64%) and uranium (10.51%) represent the main constituents with the silicate (10.94%). The traces of the iron and magnesium attributed to a background of the mica minerals. Yttrium is the sole trace element (5.34%) occupying a limited percentage of U-cote according to the similarity of ionic radii **(Fig. 24)**.

3.4.2 Zircon ($ZrSiO_4$)

The back-scattered image clarified that zircon is present as well-formed crystals of the tetragonal system **(Fig. 25)**. The spectrograph and EDX-analysis indicated that zirconium is the main constituent (45.25%) inherited with hafnium (11.76%). The presence of Hf in zircon depends on the degree of evolution of the original magma; hafnium is known to become enriched in the zircon of granitic pegmatites, especially in the late stages of the pegmatite crystallization [19]. XRD pattern of zircon, shows its characteristic peaks d-spacing (3.30, 2.52, and 4.44 A^O) matches PDF-2 Card No. (81-588).

3.4.3 Xenotime (YPO_4)

Xenotime is a yttrium phosphate mineral-enriched in rare earth elements (REE), and actinides. It can form during the late-stage activity of the hydrothermal fluids in granites or pegmatites during the cooling of its host rock [20-21]. The EDX-analysis indicates the presence of appreciable contents of Th (8.84%) and U (2.47%). XRD pattern of Xenotime, shows its characteristic peaks d-spacing (3.45, 2.56, and 1.76 A^O) matches PDF-2 Card No. (83-658) **(Fig. 26)**.

3.5. Mineralogy of (phase-II):

The El-Urf mineralized pegmatitic rocks of phase-II are characterized by an array of significant minerals comprising thorite and Meta-autunite. Nb-minerals, fluorapatite, cassiterite, atacamite, sulfide minerals, and iron oxide minerals.

3.5.1 Thorite ($(Th,U)SiO_4$

Thorite is the main radioactive mineral that is present in this phase and exists relatively more than the (phase-I). It presents as small grains, disseminated clusters, and microfracture filling. It exhibits its characteristic ESEM spectrograph and its composition is confirmed by EDX analysis, where thorium range between (38.74-49.62%) and uranium (25.82-25.54%) represent the main constituents with the silica (13.76-19.3%) and Yttrium (8.84-10.68). Some traces of iron, calcium, and aluminum were presented. **(Fig. 27)**. It is mentioned that; Thorite crystal associated with (phase-II) that has high contents of thorium and uranium **(Fig. 24)** greater than the corresponding one in (phase-I) **(Fig. 24)**. This coincides with the whole measuring e(Th) and e(U) values belong to both (phase-I) and (phase-II) pegmatite parts (table 1). XRD pattern shows its characteristic peaks d-spacing (3.56, 4.71, and 2.65 A^O) matches PDF-2 Card No. (8-395) for thorite mineral. The peak (3.31 A^O) at 2theta (26.9) may be associated with zircon mineral.

3.5.2 Nb-minerals (Columbite and Fergusonite)

Rare earth bearing minerals such as fergusonite and columbite presented in this phase. The EDX-analysis indicates the presence of appreciable contents of niobium (23.5%), yttrium (15.9), and titanium (19.94), uranium (12.47%) and thorium (4.1%). Thorite is the main radioactive mineral that is present in this mineral as minute grains included in the Nb-minerals, The EDX-analysis of these minute grains indicates the presence of thorium (47.40%) and uranium (21.59%) **(Fig. 28a)**. XRD pattern of ferrocolumbite **(Fig. 28b)**, shows its characteristic peaks d-spacing (2.96, 3.65, and 1.72 A^O) matches PDF-2 Card No. (79-1521).

3.5.3 Fluorapatite ($Ca_5(PO_4)3F$)

Fluorapatite is a Secondary hydrothermal phosphate mineral presented as an accessory mineral in pegmatite. **(Fig. 29)** shows the XRD diffractogram of fluorapatite with its main peaks (2.80, 2.70, and 2.77A^o) matching PDF_2 card No. (76-558).

3.5.4 Cassiterite (SnO)

Cassiterite is the primary ore of Tin. It forms in mid-to high-temperature hydrothermal in granite pegmatites. In this phase of pegmatite, cassiterite appears in brownish-black. The EDX-analysis indicates the presence of Tin (85.32%) **(Fig. 30)**.

3.5.4 Atacamite ($Cu_2(OH)_3Cl$)

A secondary copper mineral formed through the oxidation of other copper minerals, The EDX-analysis indicates the presence of Cupper (90.69 %) and Chlorine (9.31%) **(Fig. 31)**.

3.5.5 Sulphide minerals (Galena - Pyrite)

Base metal mineral galena (PbS) presents as visible flakes and massive cubic crystals. The EDX analysis of galena shows Pb (87.96%) and S (12.04%). Sulfide minerals occur in pegmatite as late-stage minerals. It is represented as pyrite (FeS_2) minerals associated with galena and appears in cubes and flakes of pale brassy color with a metallic luster. The EDX analysis of pyrite shows Iron up to (47.16%) with the Sulfur element (52.84) as the main component. XRD pattern of galena and pyrite, shows its

Table 1: The average of the (Tc), (eU), and (eTh) for the studied rock types.

Rock type		number of recorded readings		Av. T.C (cps)	Av. (eU) ppm	Av. (eTh) ppm	Th/U ratio
El Urf younger granite		5	Min.	45.1	1.29	3.89	2.15
			Max.	90.11	3.72	11.21	3.01
			Av.	**60.58**	**2.72**	**7.40**	**2.75**
Barren pegmatite parts		12	Min.	73.50	5.17	17.03	1.71
			Max.	146.40	9.93	21.93	3.40
			Av.	**110.41**	**7.47**	**19.19**	**2.66**
Mineralized pegmatite parts	Colorful Mineralized parts (phase-I)	7	Min.	510.83	16.74	140.1	8.37
			Max.	1460.04	40.3	459.01	11.39
			Av.	**8350.50**	**25.90**	**245.46**	**9.18**
	Opaque Mineralized parts (phase-II)	14	Min.	1524.73	29.41	692.87	21.70
			Max.	3426.10	61.58	1419.05	25.60
			Av.	**2428.62**	**45.26**	**1061.63**	**23.46**

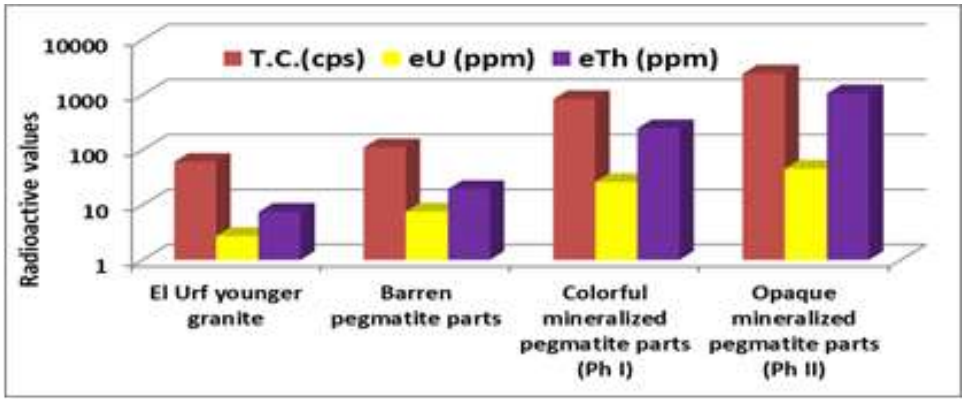

Fig.21: An illustrating histogram showing the average values of the (T.c), e(U) and e(Th) for the El Urf monzogranite and different mineralized pegmatite parts.

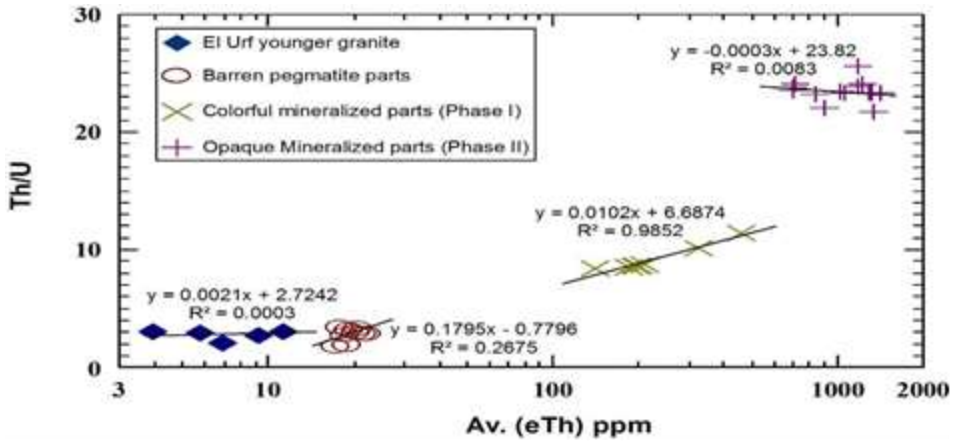

Fig. 22: eTh vs (eTh/eU) ratios for the studied rocks of G. El Urf (monzogranite and pegmatites).

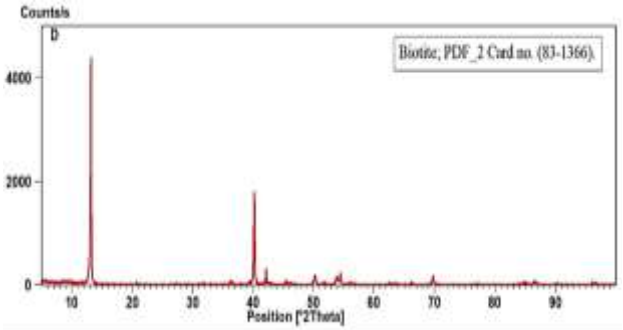

Fig. 23: XRD-diffractogram of biotite as the main mica mineral**,** El- Urf mineralized pegmatite parts (phase-I).

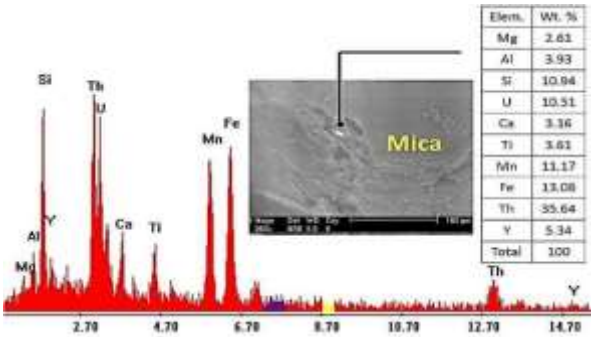

Fig. 24: ESEM-spectrograph and EDX-analysis of thorite, El-Urf mineralized pegmatite (phase-I).

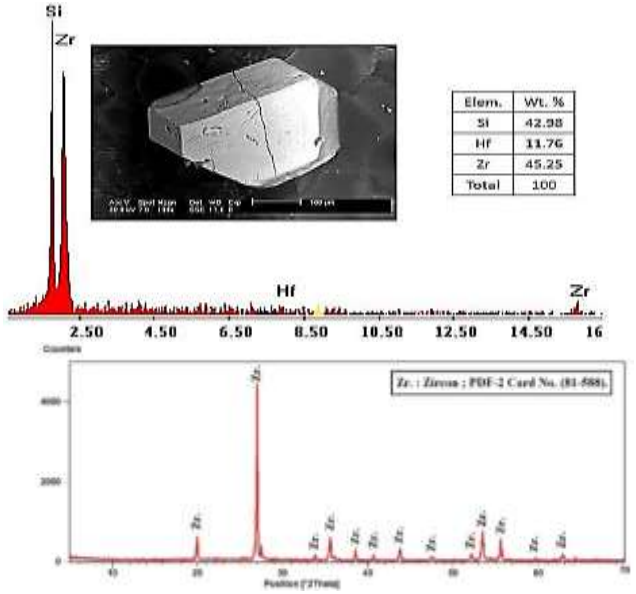

Fig. 25: ESEM-spectrograph, EDX-analysis, and XRD-diffractogram of zircon, El-Urf mineralized pegmatite (phase-I).

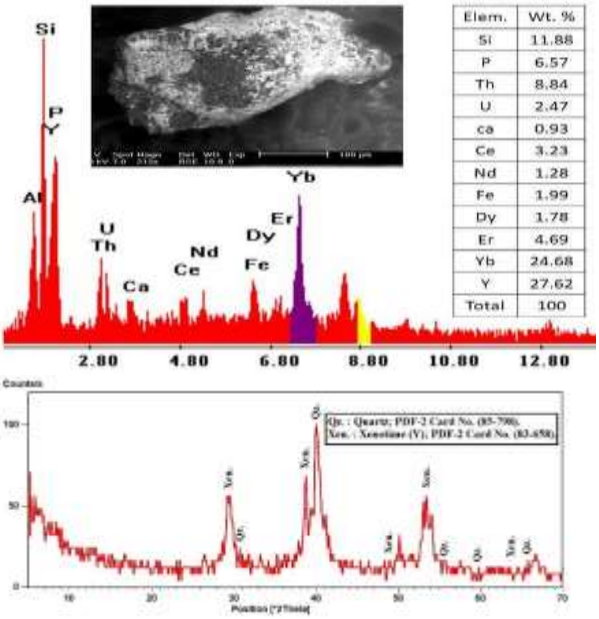

Fig. 26: ESEM-spectrograph and EDX-analysis and XRD-diffractogram of xenotime, El-Urf mineralized pegmatite parts (phase-I).

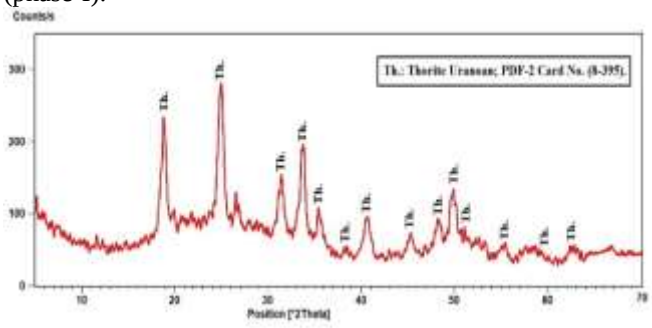

Fig. 27: ESEM-spectrograph, EDX-analysis and XRD pattern of thorite, El Urf mineralized pegmatite (phase-II).

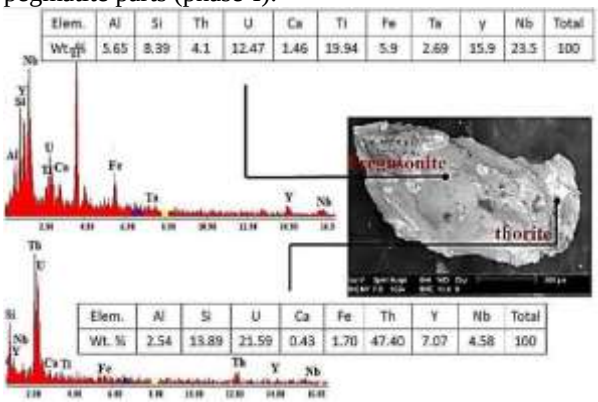

Fig. 28 (a): EDX and BSE images fergusonite and thorite

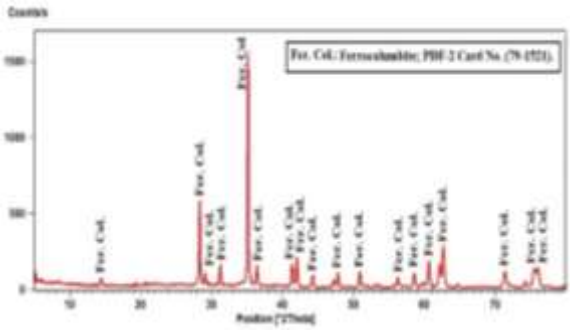

Fig.28 (b): XRD- diffractogram of Ferrocolumbite, El Urf mineralized pegmatite (phase-II).

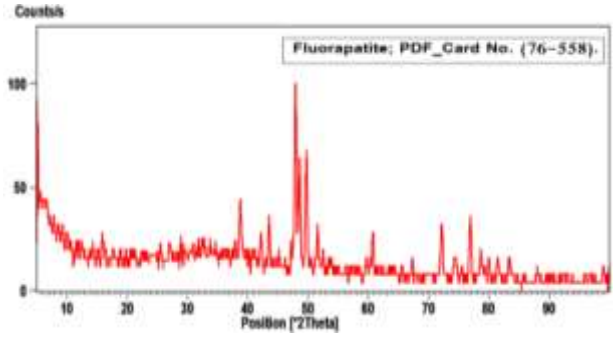

Fig. 29: XRD Pattern of Fluorapatite mineral.

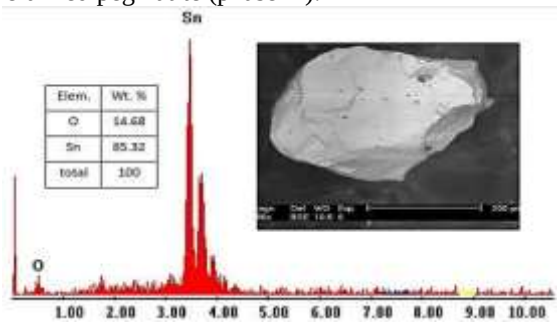

Fig.30: EDX and BSE images showing Cassiterite mineral.

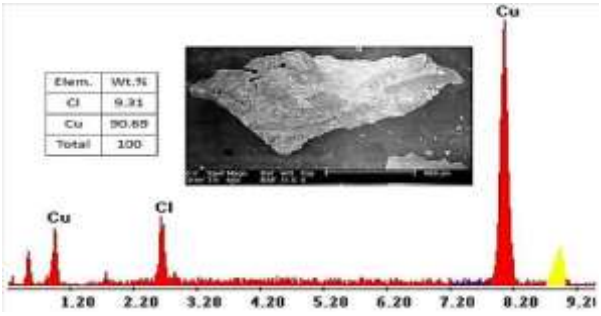

Fig. 31: EDX and BSE images showing Atacamite mineral.

characteristic peaks d-spacing (2.96, 3.42, and 2.09 A^O) matches PDF-2 Card No. (5-592) of galena. While peaks d-spacing (2.70, 1.63, and 2.42 A^O) matches PDF-2 Card No. (24-76) of pyrite **(Fig. 32)**.

3.5.6 Meta-autunite ($Ca(UO_2)_2(PO_4)_2{\cdot}6H_2O$)

Meta-autunite is a uranyl phosphate mineral that formed by dehydration of autunite that crystallized from the hydrous magma. The EDX data of meta-autunite shows U (84.21%), P (4.06%), Ca (4.08%), and Si (2.90%) are the main components. XRD pattern Meta-autunite, shows its characteristic peaks d-spacing (8.62, 3.66, and 5.42 A^O) matches PDF-2 Card No. (12-423). **(Fig. 33)**.

3.5.7 Minerals of the black fractures (iron and oxide minerals).

The black fractures found filled mainly by iron oxides. They are represented by magnetite, hematite, goethite, and ilmenite **(Fig. 34)** acting as a carrier for the uranium ions and REEs.

4 Conclusions

The studied mineralized pegmatitic rocks of the G. El Urf area could be distinguished into two phases; the first is pegmatitic rocks with colorful minerals (phase-I) and the second is pegmatitic rocks with black fractures (phase-II). The former is characterized by pegmatitic grain size smaller than the second phase of the pegmatitic rocks but coarser than the granitic rocks referring to lower fluid content rather than phase-II. It encloses accessory minerals (thorite, fluorite, zircon, and xenotime) with limited radioactivity resembling those of the granitic phase hence; it is considered as a transitional zone and maybe named pegmatitic granite. The latter (phase-II) is characterized by megacrysts of the feldspars and quartz due to a higher content of the fluids; it has another array of the accessory minerals (fluorapatite, cassiterite, atacamite, Nb-minerals, and sulfide minerals) beside the Th-minerals (thorite, uranothorite,), U-minerals (meta-autunite and uranophane) and REE-bearing minerals (pyrochlore and bastnasite). It possesses a net of fractures filled by iron oxides associated with the transported uranium and REEs. The radiometric measurements indicated two levels of radioactivity in the pegmatitic rocks.

The first (earlier) is moderately radioactive with an average eU (25.9ppm), average eTh (245.5ppm), and average Th/U ratio of about 9.48. The second (later) is anomalous with an average eU (45.26ppm), average eTh (1061.7ppm), and average Th/U ratio of about 23.46. The

two-variant relations between eTh and eTh/U indicated that the monzogranite and the Phase-II of the pegmatitic rocks are characterized by scattered relationships with nearly horizontal regression lines and low correlation coefficients while the barren pegmatitic rocks and phase-I are characterized by positive relationships with high correlation coefficients. Both of them are indicative of

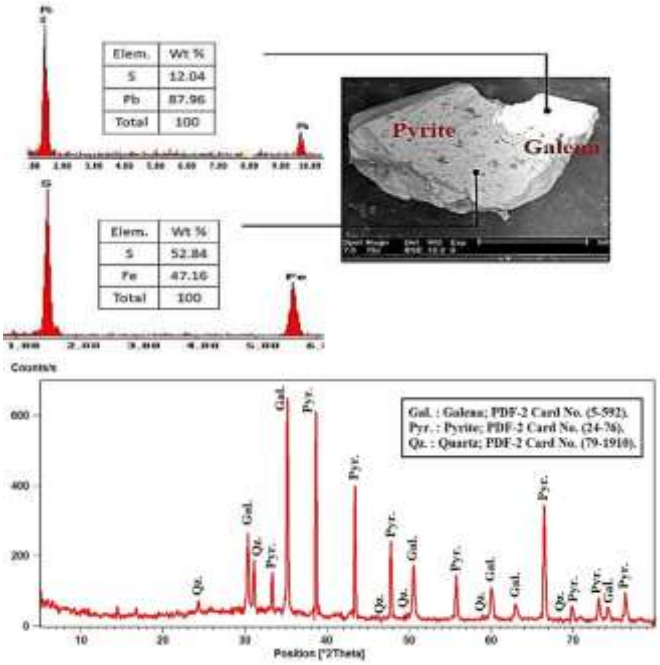

Fig. 32: EDX, BSE images, and XRD Pattern of Pyrite and Galena minerals.

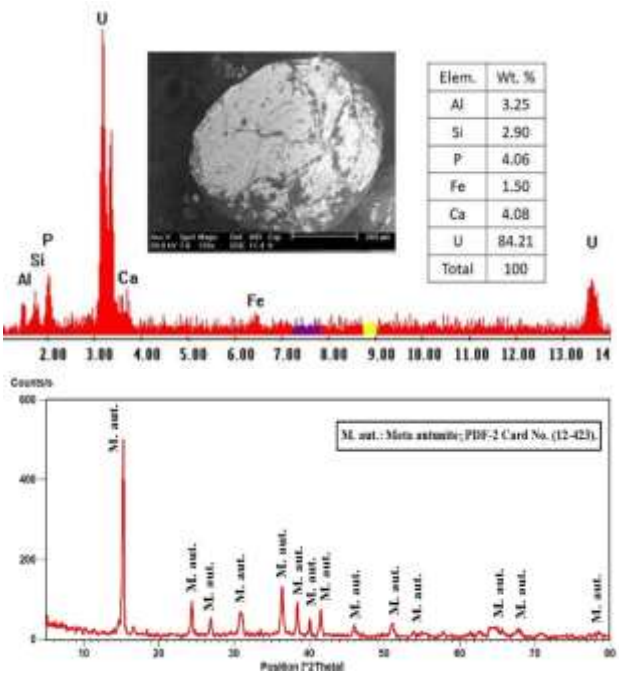

Fig. 33: EDX, BSE images, and XRD Pattern showing Meta-autunite mineral.

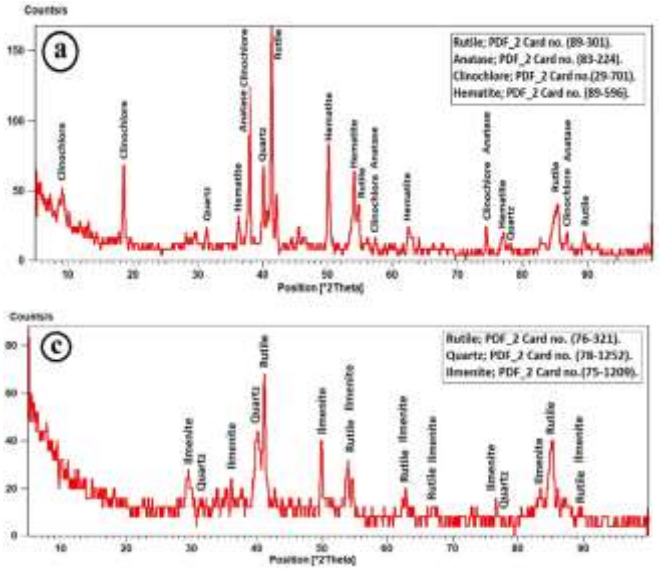

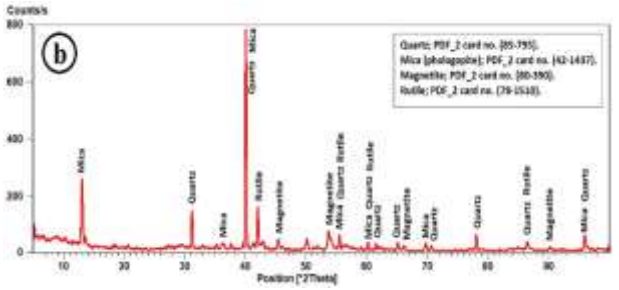

Fig. 34: Minerals of the black veinlets associating with the mineralized pegmatitic rocks of phase-II, G. El Urf area.

a) Hematite blended with rutile, anatase & clinochlore

b) Magnetite blended with rutile, mica & quartz

c) Ilmenite blended with rutile and quartz

uranium migration from the radioactive pegmatitic rocks, but the former refers to disturbance and irregular migration of uranium from these rocks while the latter refers to the regularity of uranium migration.

The radioactivity and the radioactive minerals of El Urf pegmatites are syngenetic and related to the late-stage magmatism, proved by the high Th-concentrations and presence of the radioactive minerals, followed by uranium migration. The high concentrations of thorium and the high values of Th/U ratio rather than the world (3.5)indicate that the uranium migrated from a zone to another in the same pegmatite by a circulating hydrothermal solution. Also, uranium may be transported out of the pegmatitic rocks themselves by meteoric water. The first pegmatite group may crystallize in oxidation-reduction conditions, in contrast to the second pegmatite group crystallize in highly excessive oxidation conditions and uranium migration out.

Acknowledgement

The authors thankfully acknowledge Dr. Abu Zeid E.K for performing the microscopic investigation and also indebted to Prof. Mohamed G. El Feky, Professor of Geochemistry, Nuclear Materials Authority, Egypt for supporting this work.

References

[1] A. Wataite., Petrology, geochemistry and tectonic evolution of the Pan-African rocks of Wadi Um Balad-Wadi El-Urf, North Eastern Desert, Egypt. Egy. Jour. Geol., **(41)(2B)**, 431-455, 1997.

[2] A. Moghazi., Magma source and evolution of the late Proterozoic granitiods in the Gabal El-Urf area, Eastern Desert, Egypt: Geochemical and Sr-Nd isotopic constraints. Geol. Mag., **136 (3)**, 285-300, 1999.

[3] I. Abdel Ghani., Geology, petrology, and radioactivity of Gabal El-Urf area, Central Eastern Desert, Egypt. Ph. D Thesis, Faculty of Scince, South Valley University, (Shag Branch), Egypt., 2001.

[4] D. Mostafa., Effect of the mineralogical composition and geochemical characteristics on the radioactivity of the various basement rocks at Gabal El-Dob area, Northern Eastern Desert, Egypt. Ph. D Thesis, Fac. Sci., Tanta Univ., Egypt., 2018

[5] M. El-Mansi.,and A. Dardier., Contribution to the geology and radioactivity of the older granitoids and younger granites of Gabal El-Urf-Gabal Abu Shihat area, Eastern Desert, Egypt. Delta Jour. Sci., **(29)**, 1-17. 2005.

[6] A. Asran, M. El-Mansi., M. Ibrahim., and I. Abdel Ghani., Pegmatites of Gabal El-Urf, Central Eastern Desert, Egypt, The 7th Inter. Conf. Geol. Afr., Assuit Univ., Egypt, IV.1-IV.22. 2013

[7] A. El-Sherif., Mineralogy, geochemistry and radioactive characterization of Gabal El-Urf pegmatites Central Eastern Desert. Egypt. Al-Azhar Scien Bull. (In press). 2016

[8] K. Landes., Origin and classification of pegmatites, Amer. Mineral., (18), 33- 56, 95-103, 1933.

[9] R. Jahns., and C. Burnham., Experimental studies of pegmatite genesis, In A model for the derivation and crystallization of granitic pegmatites, Econ. Geol., **(64)**, 843-64, 1969.

[10] J. Adams., and C. Weaver., Thorium to uranium ratios as indications of sedimentary processes: Example of concept of geochemical facies. Bull. Am. Assoc. Petr. Geol., **(42)**, 387–430, 1958.

[11] R. Anjos., R. Veiga., T. Soares., A. Santos., J. Aguiar., M. Frascac., J. Brage., D. Uzeda., L. Mangia, A. Facure., B. Mosquera ., C. Carvalho., and P. Gomes., Natural radionuclide distribution in Brazilian commercial granites. Radiat. Meas., **(39)**, 245–253, 2005.

[12] A. El Mezayen., M. Heikal., M. El-Feky., H. Shahin., I. Abu Zeid., S. Lasheen., Petrology, geochemistry, radioactivity, and M–W type rare earth element tetrads of El Sela altered granites, south eastern desert, Egypt. Acta Geochim., **(38)1**, 95–119, 2019.

[13] P. Macfarlane., D. Whittemore., M. Townsend., J. Doventon., V. Hamilton., W. Coyle., A. Wade., G. Macpherson., R. Black., The Dakota Aquifer Program Annual Report, FY89. Appendix B. Kansas Geological Survey, Open- File Rept., 90-27, 1989.

[14] J. Doventon., S. Prensky., Geological applications of wireline logs: a synopsis of developments and trends. Log Anal., **33(3)**, 286–303, 1992.

[15] J. Rogers., and J. Adams, Uranium and thorium, In K. H. Wedepohl (ed.), Handbook of geochemistry., Springier-Verlag, Berlin, v. 11 3, 92-B-1 to 92-0-8 and 90-Bb-1 to 90-00-5,. 201 p. 1969.

[16] H. Awad, H. Zakaly, A. Nastavkin, A. El-Taher., Radioactive content and radiological implication in granitic rocks by geochemical data and radiophysical factors, Central Eastern Desert, Egypt International Journal of Environmental Analytical Chemistry, In Press, 2020.

[17] M. Abdel-Rahman., M. Sabry, M. Khattab, A. El-Taher, S. El-Mongy., Radioactivity and risk Assessment with uncertainty treatment for analysis of black sand minerals. Zeitschrift für Anorganische und allgemeine Chemie., **647(4)**, 210-21, 2021.

[18] S. Alashrah, A. El-Taher., Assessment of natural radioactivity level and radiation hazards in soil samples of Wadi Al-Rummah Qassim province, Saudi Arabia, Journal of environmental biology., **37(5)**, 985, 2016.

[19] O. Knorring., and G. Hornung., Hafnian Zircons Nature., **(199)**, 1098—1099, 1961.

[20] E. Svecova., R. Copjakova., Z. Losos., R. Skoda., L. Nasdala., and J. Cícha., Multi-stage evolution of xenotime–(Y) from Písek pegmatites, Czech Republic, an electron probe micro-analysis and Raman spectroscopy study. DOI 10.1007/s00710-016-0442-6, 2016.

[21] D. Harlov., Formation of monazite and xenotime inclusions in fluorapatite megacrysts, Gloserheia Granite Pegmatite, Froland, Bamble Sector, southern Norway. Mineral Petrol., **(102)**, 77–86, 2011.